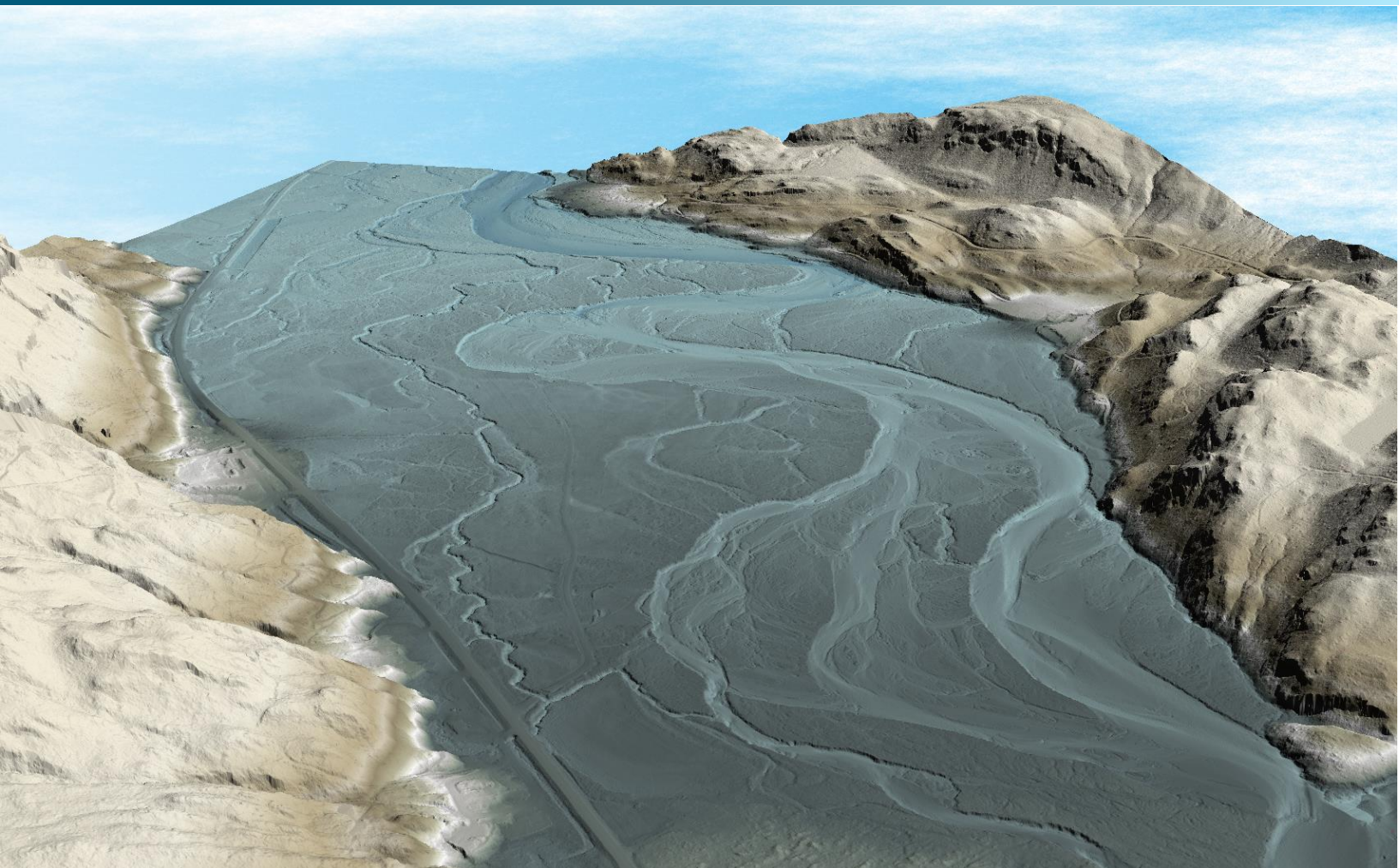


July 20, 2018



Cowlitz River, Washington Topobathymetric LiDAR Technical Data Report

Prepared For:



Abigail Gleason
Washington State Department of Natural Resources
1111 Washington Street SE, MS47007
Olympia, WA 98504
PH: 360-902-1560

Prepared By:



QSI Corvallis
1100 NE Circle Blvd., Suite 126
Corvallis, OR 97330
PH: 541-752-1204

TABLE OF CONTENTS

INTRODUCTION	1
Deliverable Products	2
ACQUISITION	4
Sensor Selection: the Riegl VQ-880-G	4
Planning.....	4
Airborne LiDAR Survey	7
Ground Control.....	9
Base Stations.....	9
Ground Survey Points (GSPs).....	10
PROCESSING	12
Topobathymetric LiDAR Data	12
Bathymetric Refraction	15
LiDAR Derived Products.....	15
Topobathymetric DEMs	15
RESULTS & DISCUSSION.....	16
Bathymetric LiDAR.....	16
Mapped Bathymetry and Depth Penetration.....	16
LiDAR Point Density.....	17
First Return Point Density.....	17
Bathymetric and Ground Classified Point Densities	17
LiDAR Accuracy Assessments	21
LiDAR Non-Vegetated Vertical Accuracy	21
Bathymetric Check Point Accuracy	24
LiDAR Relative Vertical Accuracy	26
CERTIFICATIONS	27
SELECTED IMAGES.....	28
GLOSSARY	29
APPENDIX A - ACCURACY CONTROLS	30

Cover Photo: A view looking south over the historic braided channels of the Cowlitz River near Randal, Washington. The image was created from the LiDAR bare earth model colored by elevation.

INTRODUCTION

This photo taken by QSI acquisition staff shows a view of the Cowlitz River within the Cowlitz River area of interest.



In April 2018, Quantum Spatial (QSI) was contracted by the Washington State Department of Natural Resources (WADNR) to collect topobathymetric Light Detection and Ranging (LiDAR) data in the spring of 2018 for the Cowlitz River site in Washington. The Cowlitz River area of interest stretched from the convergence of the Cowlitz River with Goat Creek upriver to the town of Packwood, Washington. Traditional near-infrared (NIR) LiDAR was fully integrated with green wavelength return data (bathymetric) LiDAR in order to provide a comprehensive topobathymetric LiDAR dataset. Data were collected to aid WADNR in assessing the channel morphology and topobathymetric surface of the study area to support river channel and fisheries restoration activities on the Cowlitz River.

This report accompanies the delivered topobathymetric LiDAR data and documents contract specifications, data acquisition procedures, processing methods, and analysis of the final dataset including LiDAR accuracy and density. Acquisition dates and acreage are shown in Table 1, a complete list of contracted deliverables provided to WADNR is shown in Table 2, and the project extent is shown in Figure 1.

Table 1: Acquisition dates, acreage, and data types collected on the Cowlitz River site

Project Site	Contracted Acres	Buffered Acres	Acquisition Dates	Data Type
Cowlitz River, Washington	20,699	22,925	04/24/2018 – 4/25/2018	Topobathymetric LiDAR

Deliverable Products

Table 2: Products delivered to WADNR for the Cowlitz River site

Cowlitz River Topobathymetric LiDAR Products	
Projection: Washington State Plane South	
Horizontal Datum: NAD83 (HARN)*	
Vertical Datum: NAVD88 (GEOID12B)	
Units: US Survey Feet	
Topobathymetric LiDAR	
Points	LAS v 1.4 <ul style="list-style-type: none"> All Classified Returns
Rasters	3.0 Foot ERDAS Imagine Files (*.img) <ul style="list-style-type: none"> Unclipped Topobathymetric Bare Earth Digital Elevation Model (DEM) Clipped Topobathymetric Bare Earth Digital Elevation Model (DEM) Highest Hit Digital Surface Model (DSM) 1.5 Foot GeoTiffs <ul style="list-style-type: none"> Green Sensor Intensity Images NIR Sensor Intensity Images 98.5 Foot ERDAS Imagine Files (*.img) <ul style="list-style-type: none"> First Return Density Raster 1,640.5 Foot ERDAS Imagine Files (*.img) <ul style="list-style-type: none"> Flightline Swath Density Raster
Vectors	Shapefiles (*.shp) <ul style="list-style-type: none"> Area of Interest LiDAR Tile Index Raster Index Bathymetric Coverage Shape Water's Edge Breaklines Smooth Best Estimate Trajectory (SBETs) Ground Survey Shapes

**The data were created in NAD83(CORS96), but for GIS purposes are defined as NAD83(HARN)*

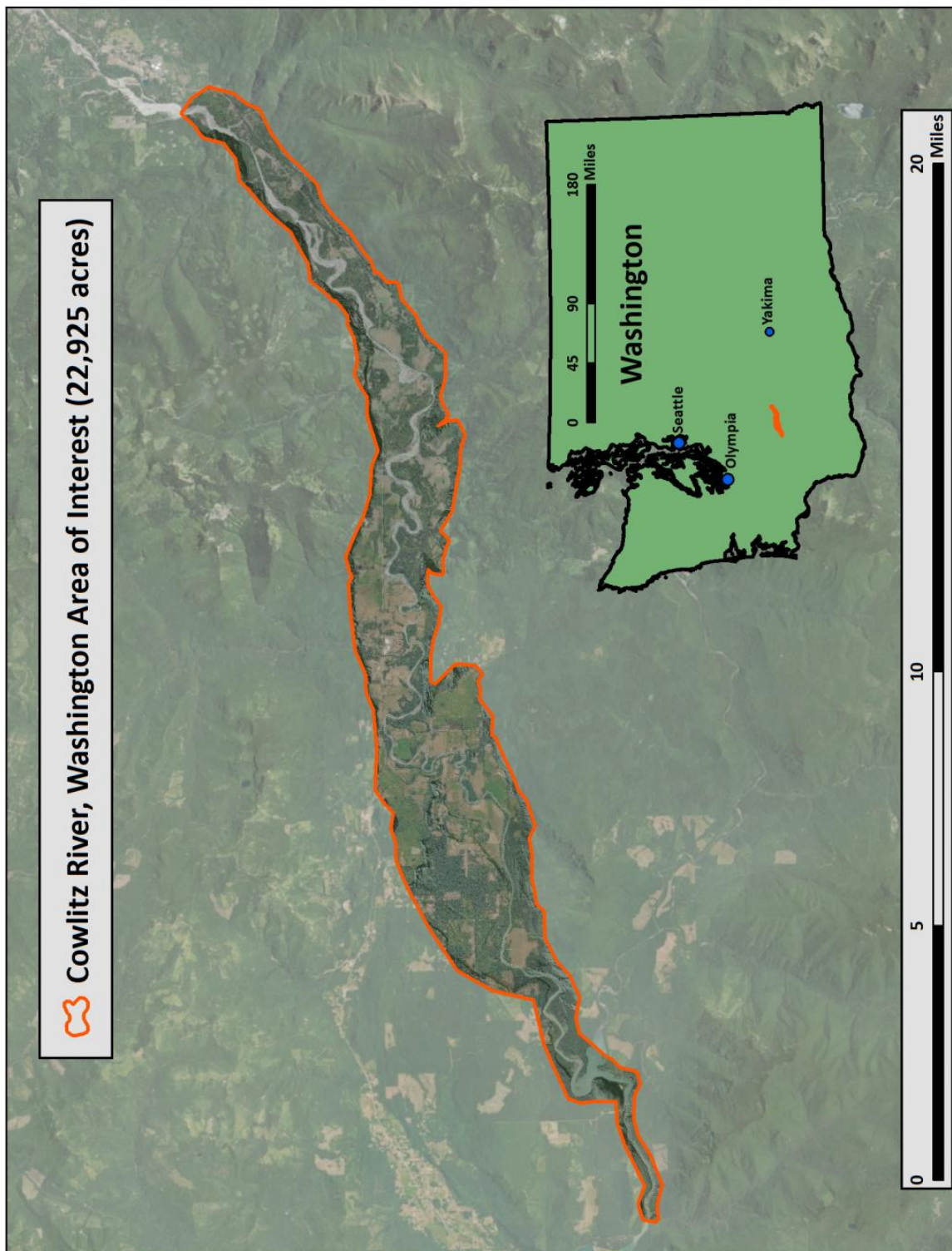


Figure 1: Location map of the Cowlitz River site in Washington

QSI's Cessna Caravan



Sensor Selection: the Riegl VQ-880-G

The Riegl VQ-880-G was selected as the hydrographic airborne laser scanner for the Cowlitz River project based on fulfillment of several considerations deemed necessary for effective mapping of the project site. A higher repetition pulse rate (up to 550 kHz), higher scanning speed, small laser footprint, and wide field of view allow for seamless collection of high resolution data of both topographic and bathymetric surfaces. A short laser pulse length allows for discrimination of underwater surface expression in shallow water, critical to shallow and dynamic environments such as the Cowlitz River. Sensor specifications and settings for the Cowlitz River acquisition are displayed in Table 3.

Planning

In preparation for data collection, QSI reviewed the project area and developed a specialized flight plan to ensure complete coverage of the Cowlitz River LiDAR study area at the cumulative target point density of ≥ 8.0 points/m² for green & NIR LiDAR returns. Acquisition parameters including orientation relative to terrain, flight altitude, pulse rate, scan angle, and ground speed were adapted to optimize flight paths and flight times while meeting all contract specifications.

Factors such as satellite constellation availability and weather windows must be considered during the planning stage. Any weather hazards or conditions affecting the flight were continuously monitored due to their potential impact on the daily success of airborne and ground operations. In addition, logistical considerations including private property access, potential air space restrictions, channel flow rates (Figure 2 and Figure 3), and water clarity were reviewed.

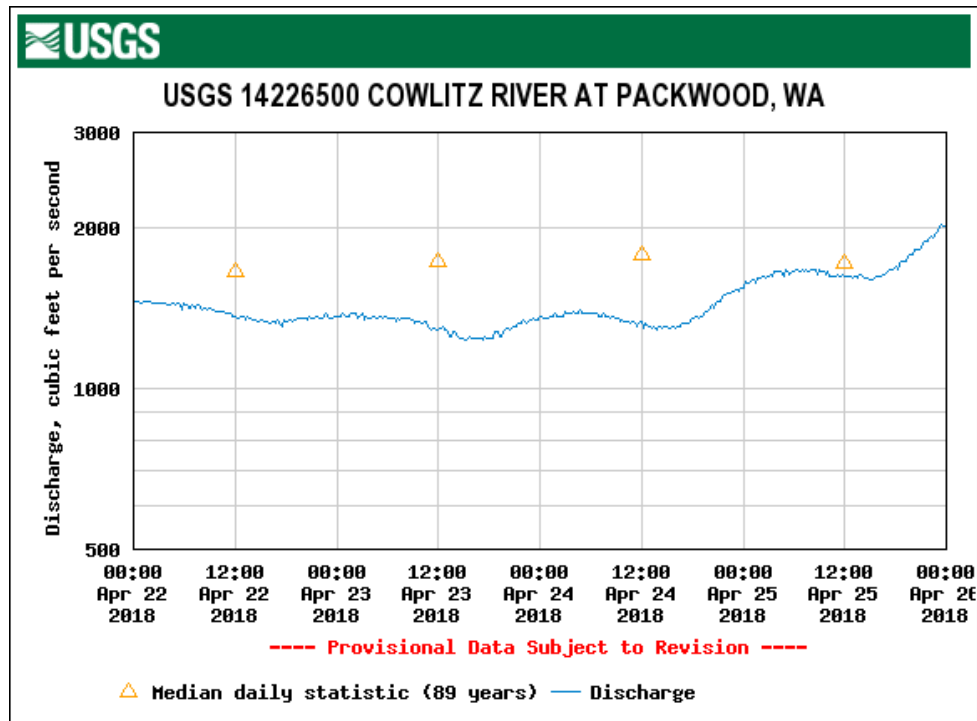


Figure 2: USGS Station 14226500 flow rates along the Cowlitz River at the time of LiDAR acquisition.

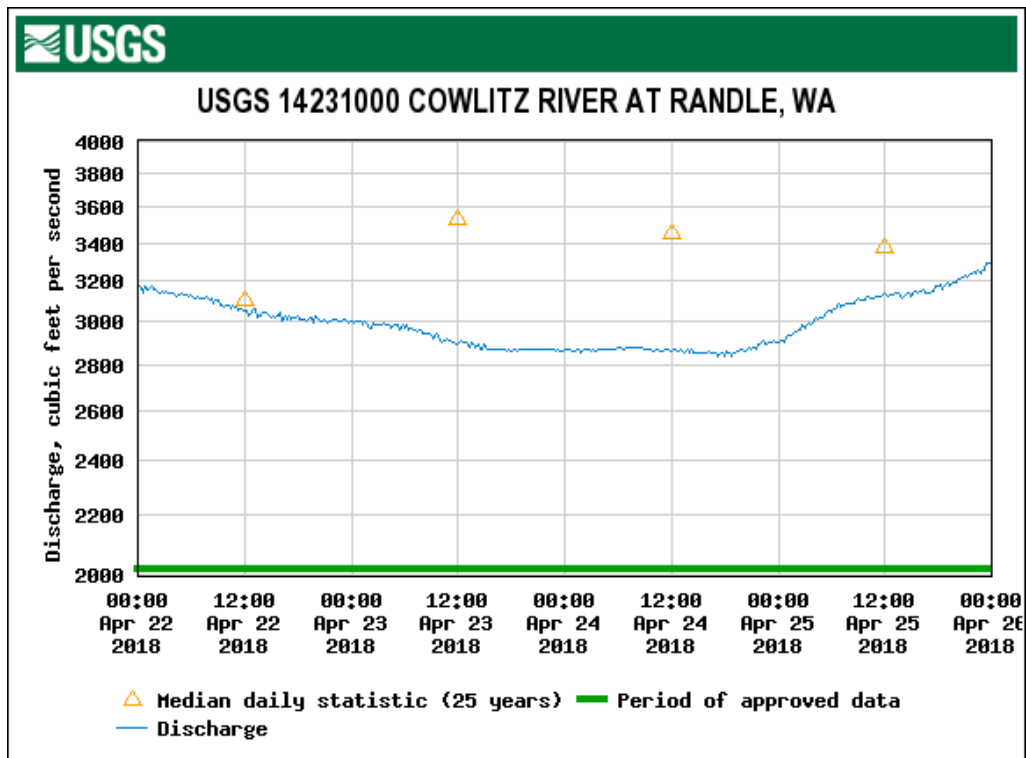


Figure 3: USGS Station 14231000 flow rates along the Cowlitz River at the time of LiDAR acquisition.



These photos taken by QSI acquisition staff display water clarity conditions at two locations within the Cowlitz River site

Airborne LiDAR Survey

The LiDAR survey was accomplished using a Riegl VQ-880-G green laser system mounted in a Cessna Caravan. The Riegl VQ-880-G uses a green wavelength ($\lambda=532$ nm) laser that is capable of collecting high resolution vegetation and topography data, as well as penetrating the water surface with minimal spectral absorption by water. The Riegl VQ-880-G also contains an integrated NIR laser ($\lambda=1064$ nm) that adds additional topography data and aids in water surface modeling. The recorded waveform enables range measurements for all discernible targets for a given pulse. The typical number of returns digitized from a single pulse range from 1 to 7 for the Cowlitz River project area. It is not uncommon for some types of surfaces (e.g., dense vegetation or water) to return fewer pulses to the LiDAR sensor than the laser originally emitted. The discrepancy between first return and overall delivered density will vary depending on terrain, land cover, and the prevalence of water bodies. All discernible laser returns were processed for the output dataset. Table 3 summarizes the settings used to yield an average pulse density of ≥ 8 pulses/m² over the Cowlitz River project area.

Table 3: LiDAR specifications and survey settings

LiDAR Survey Settings & Specifications		
Acquisition Dates	April 23 - 24, 2018	April 23 - 24, 2018
Aircraft Used	Cessna Caravan	Cessna Caravan
Sensor	Riegl	Riegl
Laser	VQ-880-G	VQ-880G-IR
Maximum Returns	Unlimited	Unlimited
Resolution/Density	8 pulses/m ²	8 pulses/m ²
Nominal Pulse Spacing	0.35 m	0.35 m
Survey Altitude (AGL)	750 m	750 m
Survey speed	120 knots	120 knots
Field of View	40°	40°
Mirror Scan Rate	80 Lines Per Second	Uniform Point Spacing
Target Pulse Rate	245 kHz	145 kHz
Pulse Length	1.5 ns	3.0 ns
Laser Pulse Footprint Diameter	52.5 cm	15 cm
Central Wavelength	532 nm	1064 nm
Pulse Mode	Multiple Times Around (MTA)	Multiple Times Around (MTA)
Beam Divergence	0.7 mrad	0.2 mrad
Swath Width	546 m	546 m
Swath Overlap	60%	60%
Intensity	16-bit	16-bit
Accuracy	RMSE _z ≤ 10 cm	RMSE _z ≤ 9 cm

All areas were surveyed with an opposing flight line side-lap of $\geq 50\%$ ($\geq 100\%$ overlap) in order to reduce laser shadowing and increase surface laser painting. To accurately solve for laser point position (geographic coordinates x, y and z), the positional coordinates of the airborne sensor and the attitude of the aircraft were recorded continuously throughout the LiDAR data collection mission. Position of the aircraft was measured twice per second (2 Hz) by an onboard differential GPS unit, and aircraft attitude was measured 200 times per second (200 Hz) as pitch, roll and yaw (heading) from an onboard inertial measurement unit (IMU). To allow for post-processing correction and calibration, aircraft and sensor position and attitude data are indexed by GPS time.

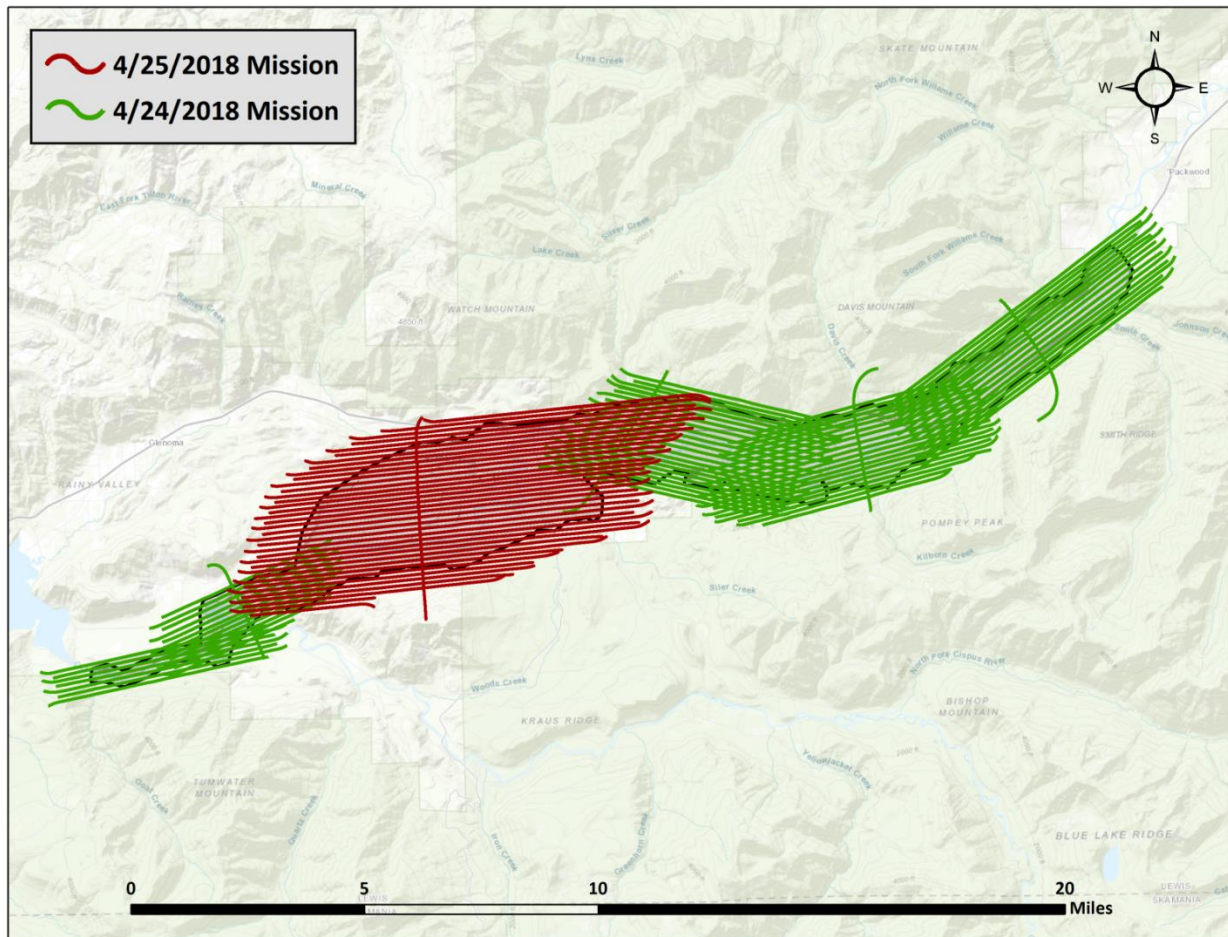


Figure 4: Cowlitz River flightline map

Ground Control

Ground control surveys, including monumentation and ground survey points (GSPs), were conducted to support the airborne acquisition. Ground control data were used to geospatially correct the aircraft positional coordinate data and to perform quality assurance checks on final LiDAR data products.

Base Stations

One permanent base station from the Washington State Reference Network (WSRN) and one station from Leica SmartNet were utilized as static base stations for the Cowlitz River airborne acquisition, providing Real-Time Network (RTN) corrections and static control within 13 nautical miles of the mission area for the LiDAR flights (Table 4, Figure 5). QSI's professional land surveyor, Evon Silvia (WAPLS#53957) oversaw and certified the ground survey.

Table 4: Base stations utilized for the Cowlitz River acquisition. Coordinates are on the NAD83 (CORS96) datum, epoch 2002.00

Monument ID	Network	Latitude	Longitude	Ellipsoid (meters)
PKWD	WSRN	46° 35' 59.25488"	-121° 40' 37.07176"	307.115
WAMO	SmartNet	46° 33' 16.78986"	-122° 16' 25.17540"	273.759

To correct the continuously recorded onboard measurements of the aircraft position, QSI utilized static Global Navigation Satellite System (GNSS) data collected at 1 Hz recording frequency by the base station. During post-processing, the static GNSS data were triangulated with nearby Continuously Operating Reference Stations (CORS) using the Online Positioning User Service (OPUS¹) to verify and update record positions as needed to align with the National Spatial Reference System (NSRS).

¹ OPUS is a free service provided by the National Geodetic Survey to process corrected monument positions.
<http://www.ngs.noaa.gov/OPUS/>.

Ground Survey Points (GSPs)

Ground survey points were collected using real time kinematic (RTK) survey techniques, in which a Real-Time Network (RTN) broadcasts corrections to a roving Trimble R6 GNSS receiver. All GSP measurements were made during periods with a Position Dilution of Precision (PDOP) of ≤ 3.0 with at least six satellites in view of the stationary and roving receivers. When collecting RTK data, the rover records data while stationary for five seconds, then calculates the pseudorange position using at least three one-second epochs. Relative errors for any GSP position must be less than 1.5 cm horizontal and 2.0 cm vertical in order to be accepted. See Table 5 for Trimble unit specifications.

GSPs were collected in areas where good satellite visibility was achieved on paved roads and other hard surfaces such as gravel or packed dirt roads. GSP measurements were not taken on highly reflective surfaces such as center line stripes or lane markings on roads due to the increased noise seen in the laser returns over these surfaces. GSPs were collected within as many flightlines as possible; however the distribution of GSPs depended on ground access constraints and monument locations and may not be equitably distributed throughout the study area (Figure 5).

Table 5: Trimble equipment identification

Receiver Model	Antenna	OPUS Antenna ID	Use
Trimble R6	Integrated GNSS Antenna R6	TRM_R6	Rover

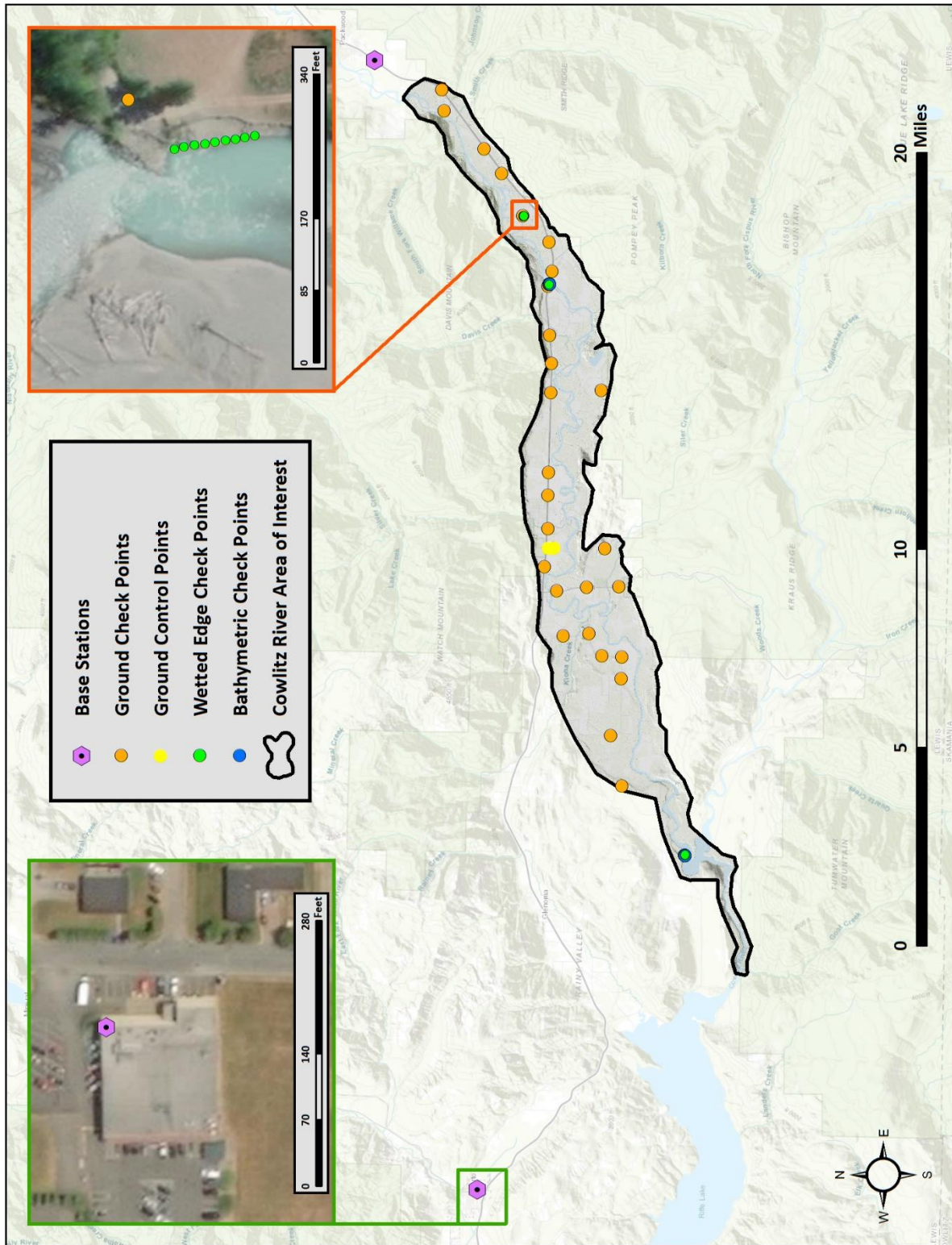
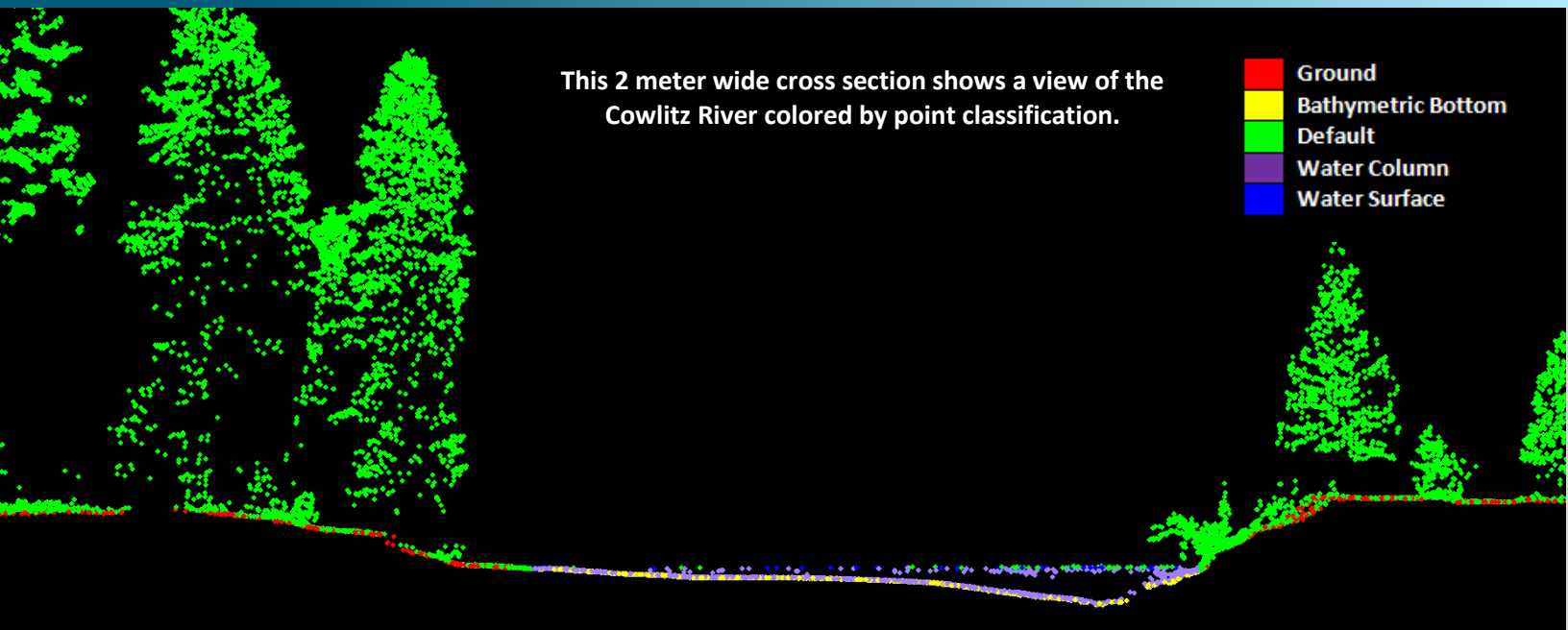


Figure 5: Ground survey location map



Topobathymetric LiDAR Data

Upon completion of data acquisition, QSI processing staff initiated a suite of automated and manual techniques to process the data into the requested deliverables. Processing tasks included GPS control computations, smoothed best estimate trajectory (SBET) calculations, kinematic corrections, calculation of laser point position, sensor and data calibration for optimal relative and absolute accuracy, and LiDAR point classification (Table 6).

Riegl's RiProcess software was used to facilitate bathymetric return processing. Once bathymetric points were differentiated, they were spatially corrected for refraction through the water column based on the angle of incidence of the laser. QSI refracted water column points using QSI's proprietary LAS processing software, Las Monkey. The resulting point cloud data were classified using both manual and automated techniques. Processing methodologies were tailored for the landscape. Brief descriptions of these tasks are shown in Table 7.

Table 6: ASPRS LAS classification standards applied to the Cowlitz River dataset

Classification Number	Classification Name	Classification Description
1	Default/Unclassified	Laser returns that are not included in the ground class, composed of vegetation and anthropogenic features
10	Default Overlap	Laser returns that are deemed not necessary to form a complete gap free coverage with respect to adjacent swaths.
2	Ground	Laser returns that are determined to be ground using automated and manual cleaning algorithms
7W	Noise	Laser returns that are often associated with birds, scattering from reflective surfaces, or artificial points below the ground surface
9	NIR Water Surface	NIR laser returns that are determined to be water using automated and manual cleaning algorithms
17	Bridge	Bridge decks
40	Bathymetric Bottom	Refracted Riegl sensor returns that fall within the water's edge breakline which characterize the submerged topography.
41	Water Surface	Green laser returns that are determined to be water surface points using automated and manual cleaning algorithms.
45	Water Column	Refracted Riegl sensor returns that are determined to be water using automated and manual cleaning algorithms.

Table 7: LiDAR processing workflow

LiDAR Processing Step	Software Used
Resolve kinematic corrections for aircraft position data using kinematic aircraft GPS and static ground GPS data. Develop a smoothed best estimate of trajectory (SBET) file that blends post-processed aircraft position with sensor head position and attitude recorded throughout the survey.	POSPac MMS v.8.2
Calculate laser point position by associating SBET position to each laser point return time, scan angle, intensity, etc. Create raw laser point cloud data for the entire survey in *.las (ASPRS v. 1.4) format. Convert data to orthometric elevations by applying a geoid correction.	RiProcess v1.8.5 TerraMatch v.18
Import raw laser points into manageable blocks to perform manual relative accuracy calibration and filter erroneous points. Classify ground points for individual flight lines.	TerraScan v.18
Using ground classified points per each flight line, test the relative accuracy. Perform automated line-to-line calibrations for system attitude parameters (pitch, roll, heading), mirror flex (scale) and GPS/IMU drift. Calculate calibrations on ground classified points from paired flight lines and apply results to all points in a flight line. Use every flight line for relative accuracy calibration.	TerraMatch v.18
Apply refraction correction to all subsurface returns.	Las Monkey 2.3 (QSI proprietary)
Classify resulting data to ground and other client designated ASPRS classifications (Table 6). Assess statistical absolute accuracy via direct comparisons of ground classified points to ground control survey data.	TerraScan v.18 TerraModeler v.18
Generate bare earth models as triangulated surfaces. Generate highest hit models as a surface expression of all classified points. Export all surface models in ERDAS Imagine (.img) format at a 3.0 foot pixel resolution.	TerraScan v.18 TerraModeler v.18 ArcMap v. 10.3.1
Correct intensity values for variability and export intensity images as GeoTIFFs at a 1.5 foot pixel resolution.	TerraScan v.18 TerraModeler v.18 ArcMap v. 10.3.1 Las Product Creator v.3.0 (QSI proprietary)

Bathymetric Refraction

The water surface model used for refraction is generated using NIR points within the breaklines defining the water's edge. Points are filtered and edited to obtain the most accurate representation of the water surface and are used to create a water surface model TIN. A tin model is preferable to a raster based water surface model to obtain the most accurate angle of incidence during refraction. The refraction processing is done using Las Monkey; QSI's proprietary LiDAR processing tool. After refraction, the points are compared against bathymetric control points to assess accuracy.

LiDAR Derived Products

Because hydrographic laser scanners penetrate the water surface to map submerged topography, this affects how the data should be processed and presented in derived products from the LiDAR point cloud. The following discusses certain derived products that vary from the traditional (NIR) specification and delivery format.

Topobathymetric DEMs

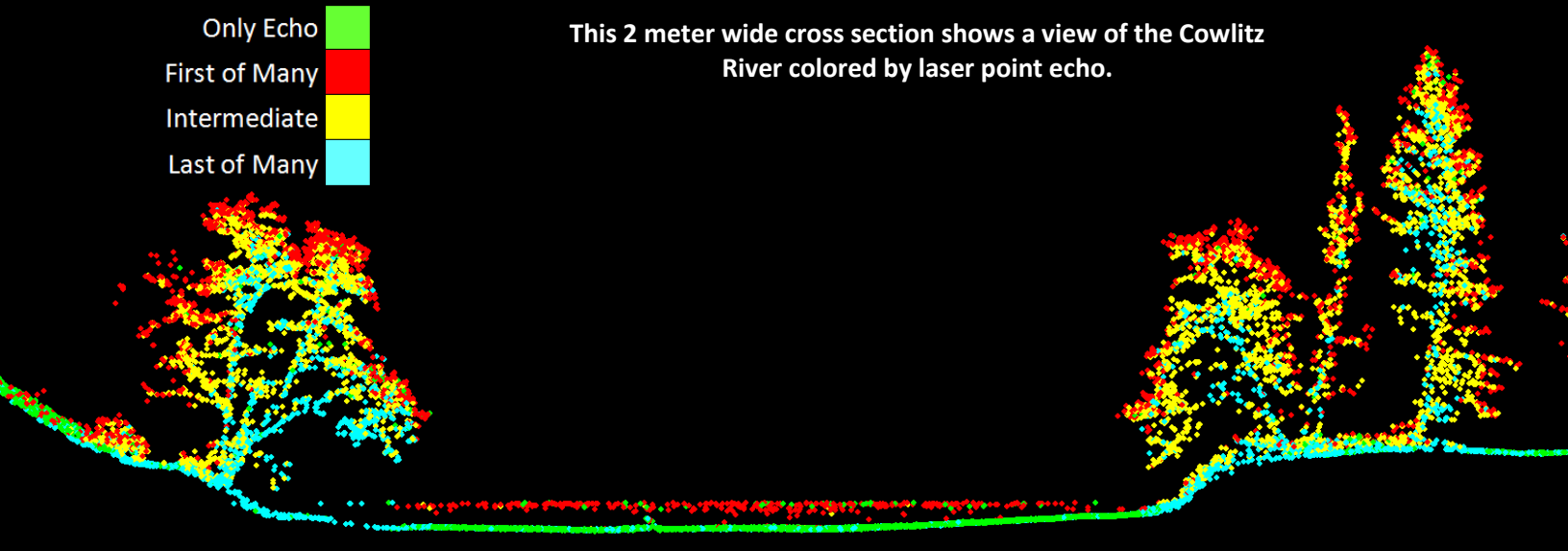
Bathymetric bottom returns can be limited by depth, water clarity, and bottom surface reflectivity. Water clarity and turbidity affects the depth penetration capability of the green wavelength laser with returning laser energy diminishing by scattering throughout the water column. Additionally, the bottom surface must be reflective enough to return remaining laser energy back to the sensor at a detectable level. Although the predicted depth penetration range of the Riegl VQ-880-G sensor is 1.5 Secchi depths on brightly reflective surfaces, it is not unexpected to have no bathymetric bottom returns in turbid or non-reflective areas.

As a result, creating digital elevation models (DEMs) presents a challenge with respect to interpolation of areas with no returns. Traditional DEMs are "unclipped", meaning areas lacking ground returns are interpolated from neighboring ground returns (or breaklines in the case of hydro-flattening), with the assumption that the interpolation is close to reality. In bathymetric modeling, these assumptions are prone to error because a lack of bathymetric returns can indicate a change in elevation that the laser can no longer map due to increased depths. The resulting void areas may suggest greater depths, rather than similar elevations from neighboring bathymetric bottom returns. Therefore, QSI created a water polygon with bathymetric coverage to delineate areas with successfully mapped bathymetry. This shapefile was used to control the extent of the delivered clipped topobathymetric model to avoid false triangulation (interpolation from TIN'ing) across areas in the water with no bathymetric returns.

RESULTS & DISCUSSION

Only Echo
First of Many
Intermediate
Last of Many

This 2 meter wide cross section shows a view of the Cowlitz River colored by laser point echo.



Bathymetric LiDAR

An underlying principle for collecting hydrographic LiDAR data is to survey near-shore areas that can be difficult to collect with other methods, such as multi-beam sonar, particularly over large areas. In order to determine the capability and effectiveness of the bathymetric LiDAR QSI considered bathymetric return densities and spatial accuracy.

Mapped Bathymetry and Depth Penetration

The specified depth penetration range of the Riegl VQ-880-G sensor is 1.5 secchi depths; therefore, bathymetry data below 1.5 secchi depths at the time of acquisition is not to be expected. To assist in evaluating performance results of the sensor, a polygon layer was created to delineate areas where bathymetry was successfully mapped.

This shapefile was used to control the extent of the delivered clipped topo-bathymetric model and to avoid false triangulation across areas in the water with no returns. Insufficiently mapped areas were identified by triangulating bathymetric bottom points with an edge length maximum of 15.2 feet (4.56 meters). This ensured all areas of no returns $>100 \text{ ft}^2$ ($> 9 \text{ m}^2$), were identified as data voids. Overall, QSI mapped 67.5% of the bathymetry within the Cowlitz River project area.

LiDAR Point Density

First Return Point Density

The acquisition parameters were designed to acquire an average first-return density of 8 points/m². First return density describes the density of pulses emitted from the laser that return at least one echo to the system. Multiple returns from a single pulse were not considered in first return density analysis. Some types of surfaces (e.g., breaks in terrain, water and steep slopes) may have returned fewer pulses than originally emitted by the laser.

First returns typically reflect off the highest feature on the landscape within the footprint of the pulse. In forested or urban areas the highest feature could be a tree, building or power line, while in areas of unobstructed ground, the first return will be the only echo and represents the bare earth surface.

The average first-return density of the Cowlitz River LiDAR project was 2.52 points/ft² (27.14 points/m²) (Table 8). The statistical and spatial distributions of all first return densities per 100 m x 100 m cell are portrayed in Figure 6 and Figure 9.

Bathymetric and Ground Classified Point Densities

The density of ground classified LiDAR returns and bathymetric bottom returns were also analyzed for this project. Terrain character, land cover, and ground surface reflectivity all influenced the density of ground surface returns. In vegetated areas, fewer pulses may have penetrated the canopy, resulting in lower ground density. Similarly, the density of bathymetric bottom returns was influenced by turbidity, depth, and bottom surface reflectivity. In turbid areas, fewer pulses may have penetrated the water surface, resulting in lower bathymetric density.

The ground and bathymetric bottom classified density of LiDAR data for the Cowlitz River project was 0.30 points/ft² (3.26 point/m²) (Table 8). The statistical and spatial distributions ground classified and bathymetric bottom return densities per 100 m x 100 m cell are portrayed in Figure 7 and Figure 9.

Additionally, for the Cowlitz River project, density values of only bathymetric bottom returns were calculated for areas containing at least one bathymetric bottom return. Areas lacking bathymetric returns (voids) were not considered in calculating an average density value. Within the successfully mapped area, a bathymetric bottom return density of 0.26 point/ft² (2.87 points/m²) was achieved.

Table 8: Average LiDAR point densities

Density Type	Point Density
Green & NIR Lasers First Returns	2.52 points/ft ² 27.14 points/m ²
Ground and Bathymetric Bottom Classified Returns	0.30 points/ft ² 3.26 points/m ²
Bathymetric Bottom Classified Returns	0.26 points/ft ² 2.87 points/m ²

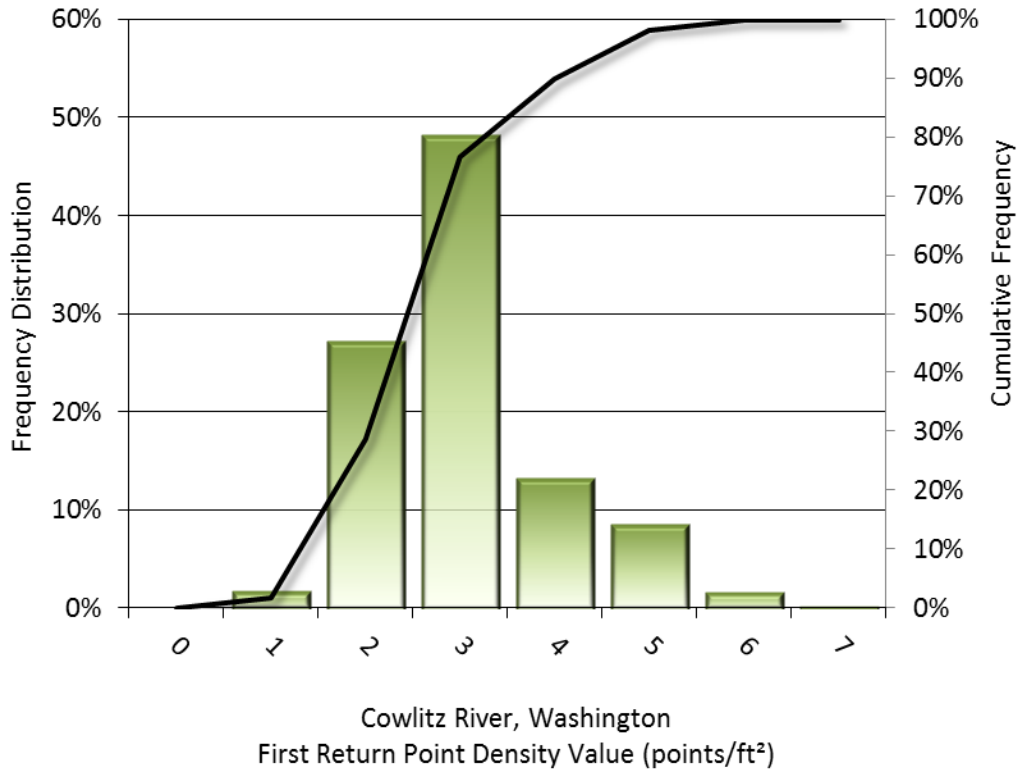


Figure 6: Frequency distribution of first return densities per 100 x 100 m cell

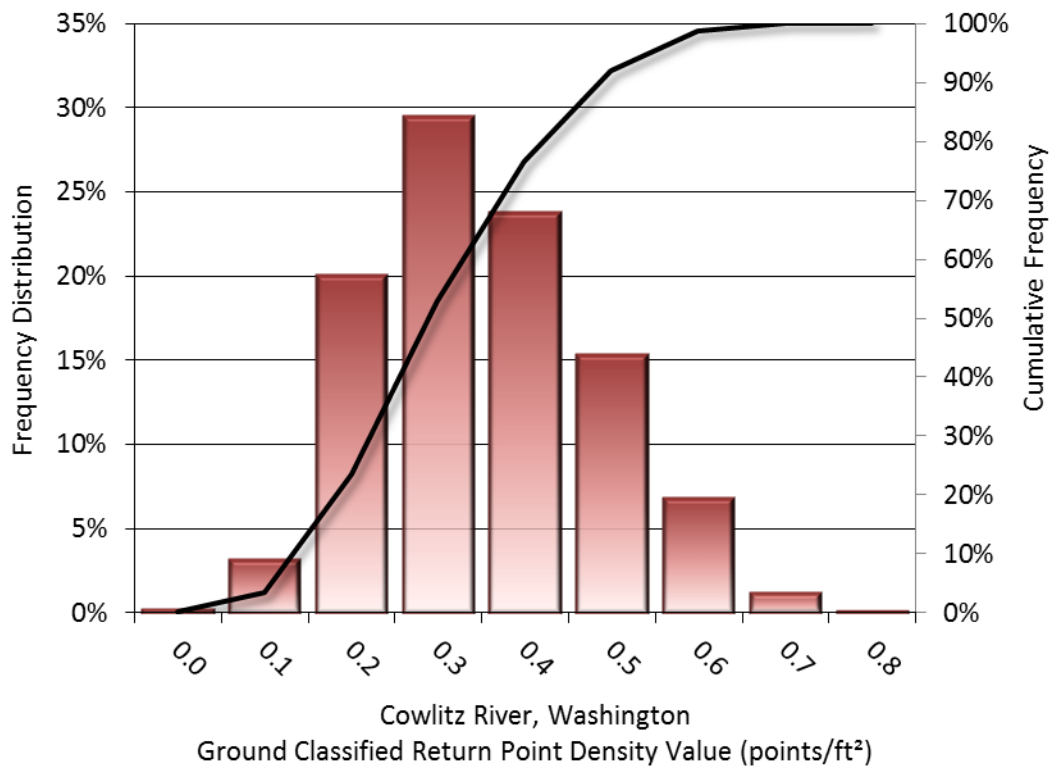


Figure 7: Frequency distribution of ground and bathymetric bottom classified return densities per 100 x 100 m cell

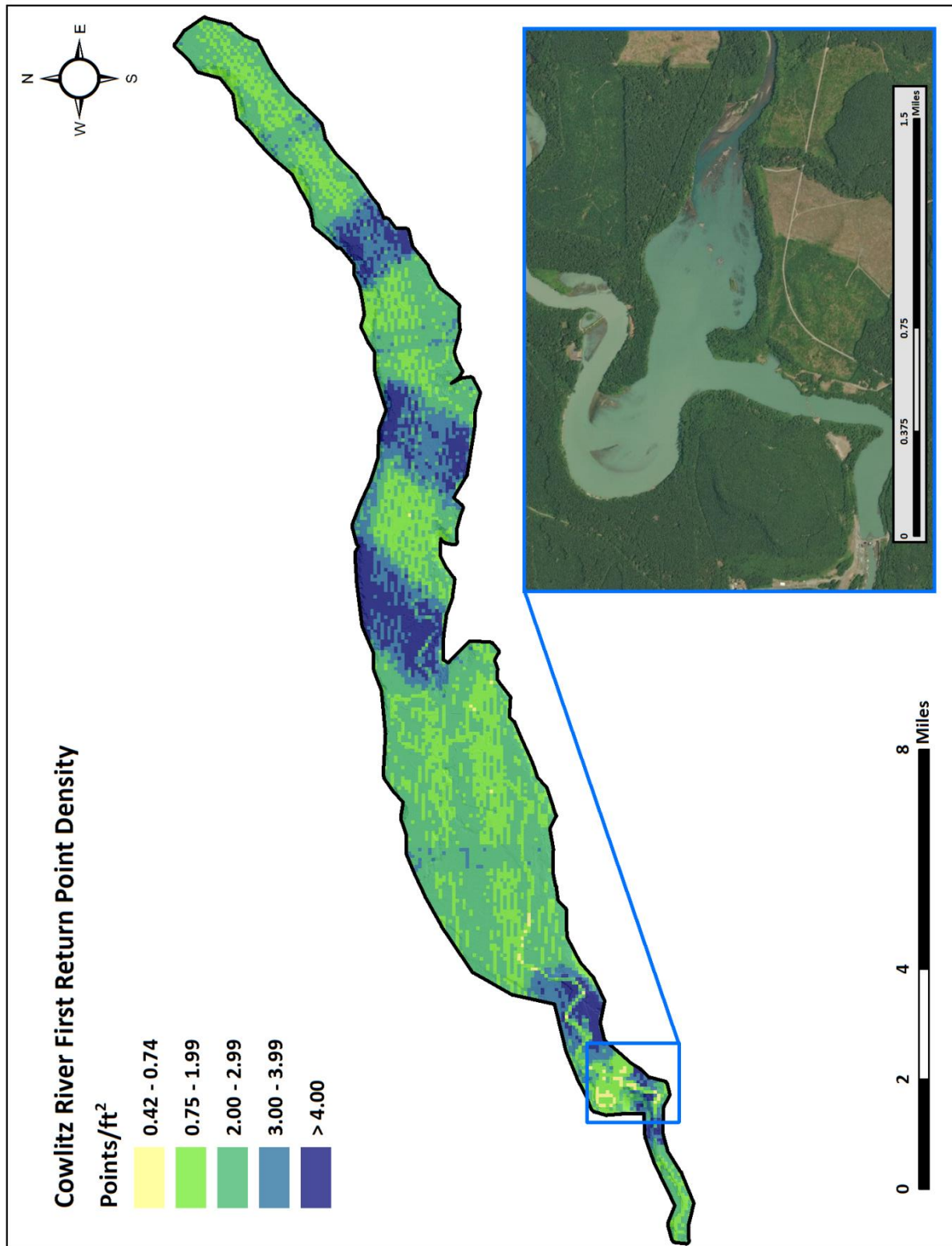


Figure 8: First return point density map for the Cowlitz river site (100 m x 100 m cells)

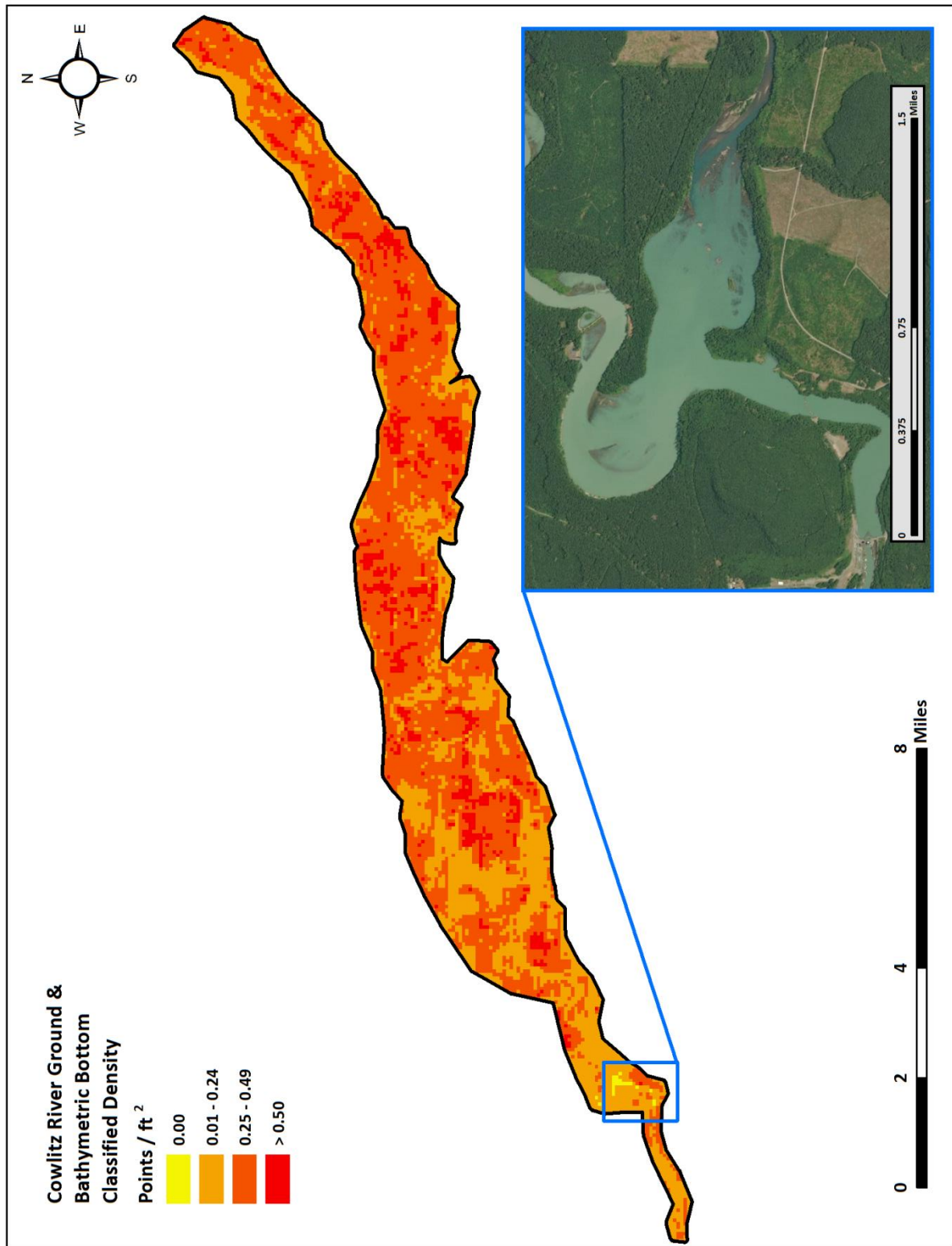


Figure 9: Ground and bathymetric bottom density map for the Cowlitz River site (100 m x 100 m cells)

LiDAR Accuracy Assessments

The accuracy of the LiDAR data collection can be described in terms of absolute accuracy (the consistency of the data with external data sources) and relative accuracy (the consistency of the dataset with itself). See Appendix A for further information on sources of error and operational measures used to improve relative accuracy.

LiDAR Non-Vegetated Vertical Accuracy

Absolute accuracy was assessed using Non-vegetated Vertical Accuracy (NVA) reporting designed to meet guidelines presented in the FGDC National Standard for Spatial Data Accuracy². NVA compares known ground quality assurance point data collected on open, bare earth surfaces with level slope (<20°) to the triangulated surface generated by the LiDAR points. NVA is a measure of the accuracy of LiDAR point data in open areas where the LiDAR system has a high probability of measuring the ground surface and is evaluated at the 95% confidence interval ($1.96 * RMSE$), as shown in Table 9.

The mean and standard deviation (sigma σ) of divergence of the ground surface model from ground check point coordinates are also considered during accuracy assessment. These statistics assume the error for x, y and z is normally distributed, and therefore the skew and kurtosis of distributions are also considered when evaluating error statistics. For the Cowlitz River survey, 29 ground check points were withheld from the calibration and post-processing of the LiDAR point cloud, with resulting non-vegetated vertical accuracy of 0.144 feet (0.044 meters) as compared to the unclassified LAS point cloud and 0.165 feet (0.050 m) as compared to the bare earth DEM, with 95% confidence.

QSI also assessed absolute accuracy using 75 ground control points. Although these points were used in the calibration and post-processing of the LiDAR point cloud, they still provide a good indication of the overall accuracy of the LiDAR dataset, and therefore have been provided in Table 9 and Figure 12.

² Federal Geographic Data Committee, ASPRS POSITIONAL ACCURACY STANDARDS FOR DIGITAL GEOSPATIAL DATA EDITION 1, Version 1.0, NOVEMBER 2014. <http://www.asprs.org/PAD-Division/ASPRS-POSITIONAL-ACCURACY-STANDARDS-FOR-DIGITAL-GEOSPATIAL-DATA.html>.

Table 9: Absolute accuracy (NVA) results

Non-Vegetated Vertical Accuracy			
	Ground Check Points (Unclassified LAS)	Ground Check Points (Bare Earth DEM)	Ground Control Points
Sample	29 points	29 points	75 points
NVA (1.96*RMSE)	0.144 ft	0.165 ft	0.077 ft
	0.044 m	0.050 m	0.023 m
Average	0.034 ft	-0.043 ft	0.000 ft
	0.010 m	-0.013 m	0.000 m
Median	0.023 ft	-0.049 ft	0.003 ft
	0.007 m	-0.015 m	0.001 m
RMSE	0.073 ft	0.084 ft	0.039 ft
	0.022 m	0.026 m	0.012 m
Standard Deviation (1 σ)	0.066 ft	0.073 ft	0.039 ft
	0.020 m	0.022 m	0.012 m

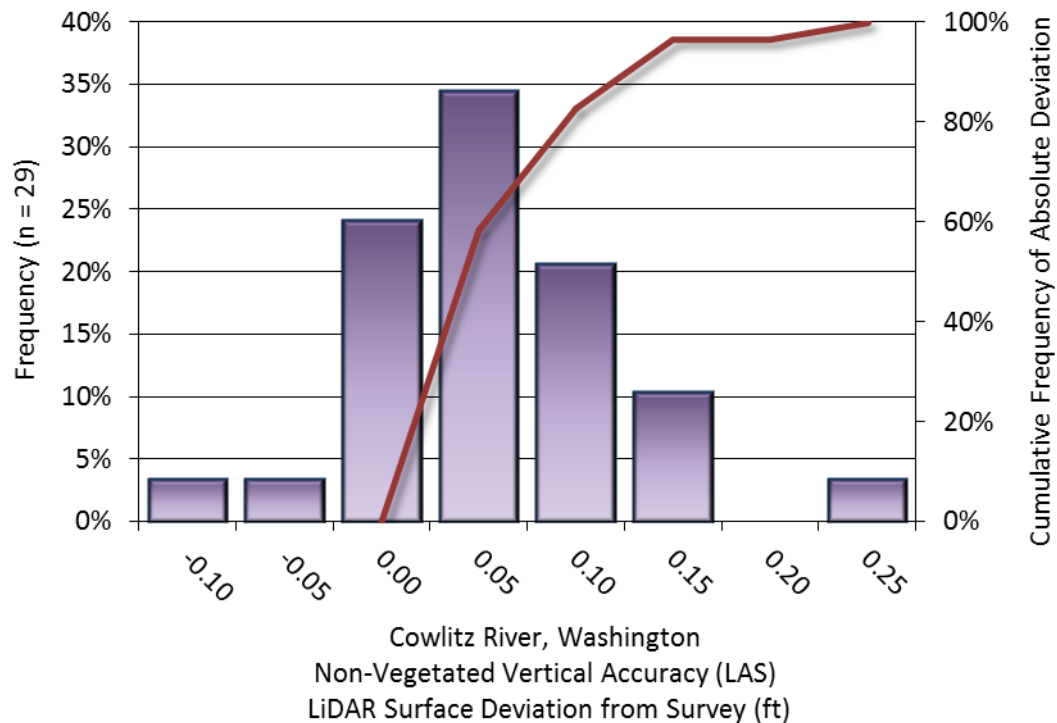


Figure 10: Frequency histogram for LiDAR surface deviation from ground check point values as compared to the unclassified LAS point cloud

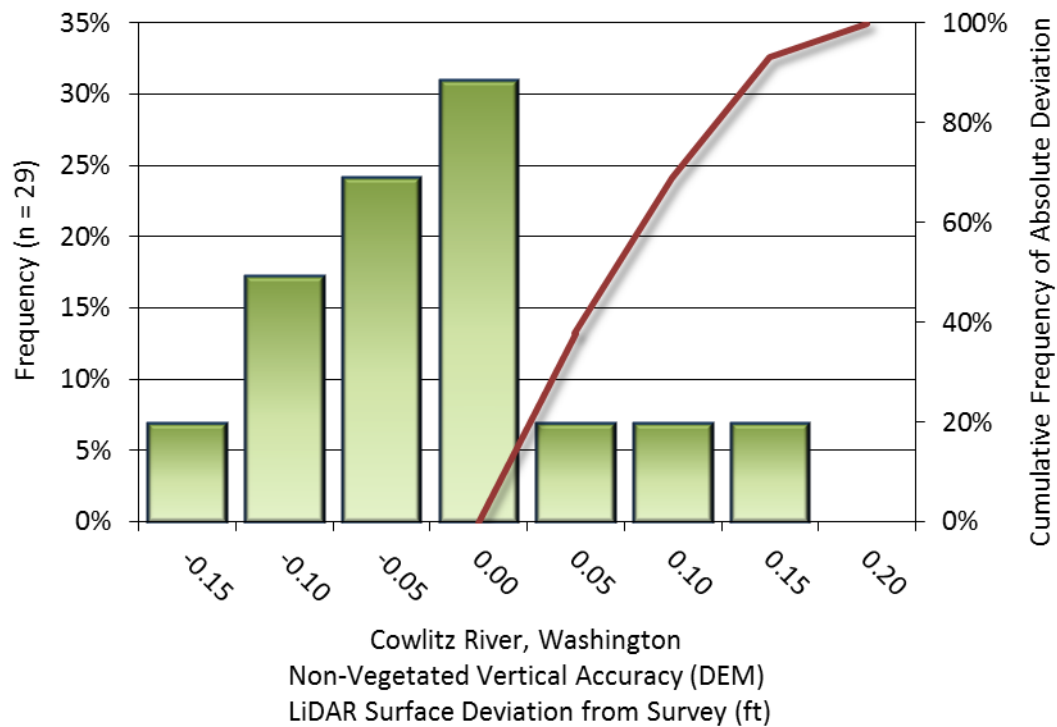


Figure 11: Frequency histogram for LiDAR surface deviation from ground check point values as compared to the bare earth DEM

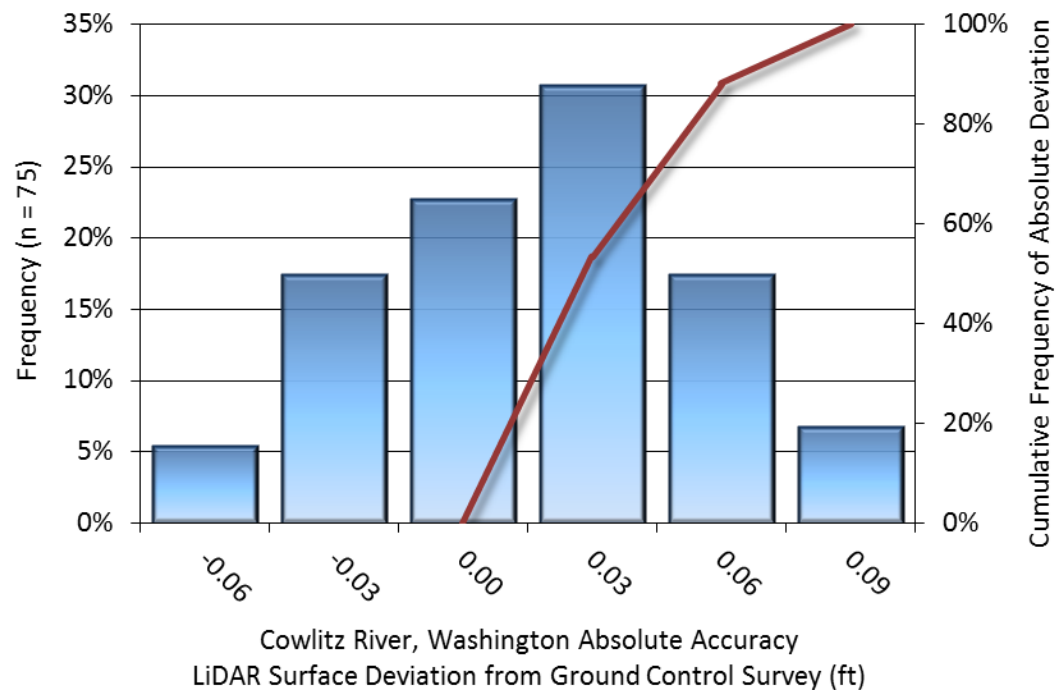


Figure 12: Frequency histogram for LiDAR surface deviation ground control point values

Bathymetric Check Point Accuracy

Bathymetric (submerged or along the water's edge) check points were also collected in order to assess the vertical accuracy of the bathymetric surface. Assessment of 26 submerged bathymetric check points resulted in a vertical accuracy of 0.180 feet (0.055 meters), evaluated at the 95th percentile. Additionally, assessment of 22 wetted edge check points resulted in a vertical accuracy of 0.353 feet (0.108 meters), evaluated at the 95th percentile (Table 10, Figure 13, and Figure 14).

Table 10: Bathymetric Vertical Accuracy for the Cowlitz River Project

Bathymetric Vertical Accuracy		
	Submerged Bathymetric Check Points	Wetted Edge Bathymetric Check Points
Sample	26 points	22 points
95 th Percentile	0.180 ft 0.055 m	0.353 ft 0.108 m
Average	-0.019 ft -0.006 m	0.131 ft 0.040 m
Median	-0.026 ft -0.008 m	0.107 ft 0.033 m
RMSE	0.091 ft 0.028 m	0.193 ft 0.059 m
Standard Deviation (1σ)	0.091 ft 0.028 m	0.145 ft 0.044 m

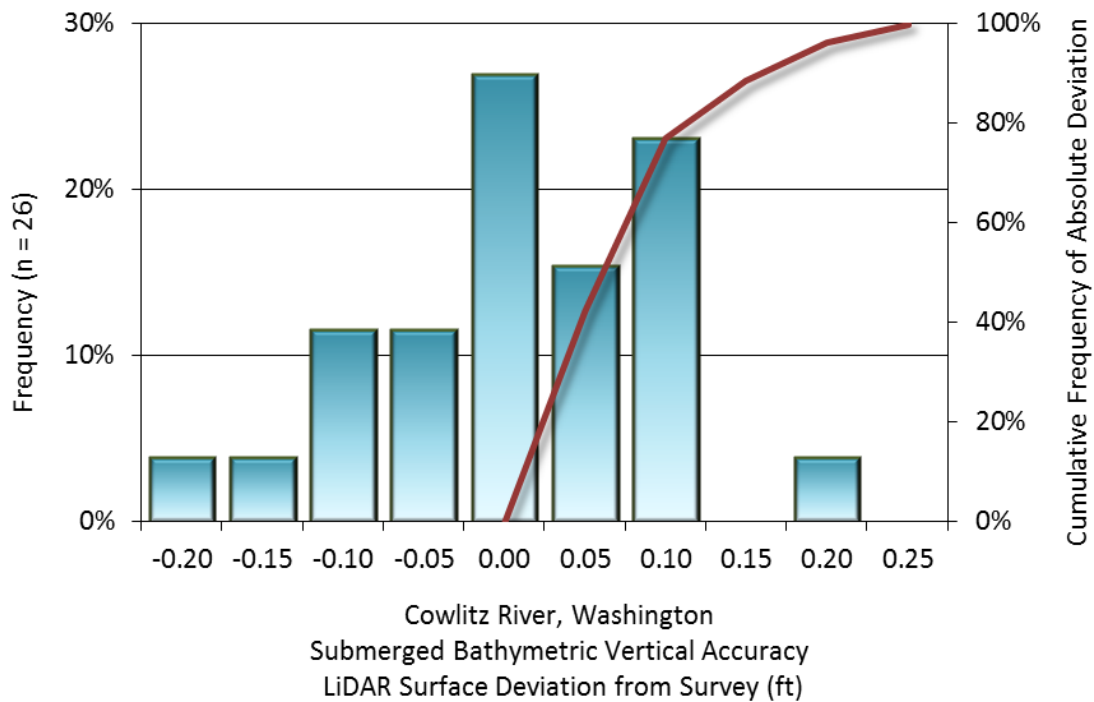


Figure 13: Frequency histogram for LiDAR surface deviation from submerged bathymetric check point values

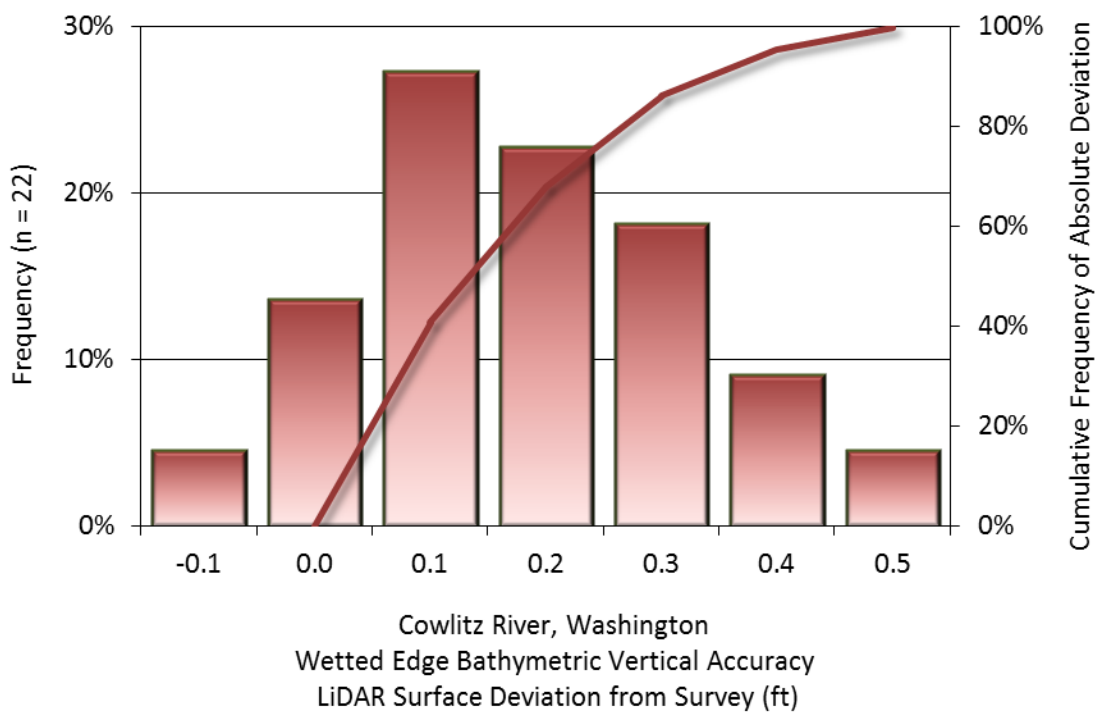


Figure 14: Frequency histogram for LiDAR surface deviation from wetted edge check point values

LiDAR Relative Vertical Accuracy

Relative vertical accuracy refers to the internal consistency of the data set as a whole: the ability to place an object in the same location given multiple flight lines, GPS conditions, and aircraft attitudes. When the LiDAR system is well calibrated, the swath-to-swath vertical divergence is low (<0.10 meters). The relative vertical accuracy was computed by comparing the ground surface model of each individual flight line with its neighbors in overlapping regions. The average (mean) line to line relative vertical accuracy for the Cowlitz River LiDAR project was 0.118 feet (0.036 meters) (Table 11, Figure 15).

Table 11: Relative accuracy results

Relative Accuracy	
Sample	239 surfaces
Average	0.118 ft 0.036 m
Median	0.122 ft 0.037 m
RMSE	0.140 ft 0.043 m
Standard Deviation (1 σ)	0.033 ft 0.010 m
1.96 σ	0.066 ft 0.020 m

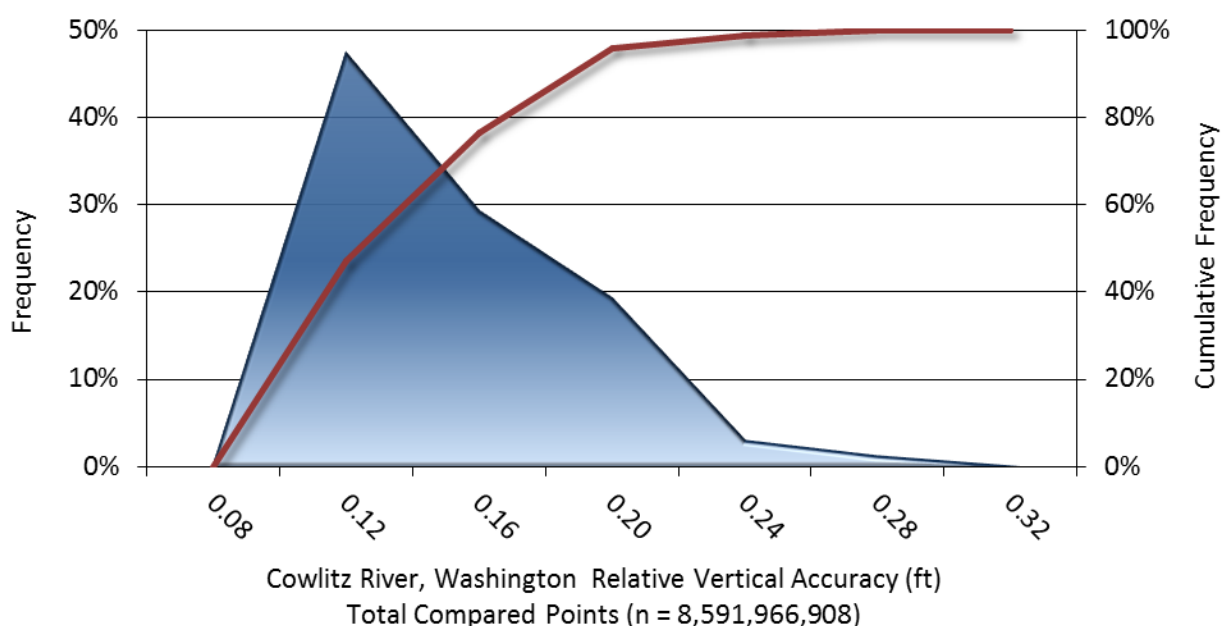


Figure 15: Frequency plot for relative vertical accuracy between flight lines

CERTIFICATIONS

Quantum Spatial, Inc. provided LiDAR services for the Cowlitz River project as described in this report.

I, Tucker Selko, have reviewed the attached report for completeness and hereby state that it is a complete and accurate report of this project.

Tucker Selko
Tucker Selko (Jul 19, 2018)

Jul 19, 2018

Tucker Selko
Project Manager
Quantum Spatial, Inc.

I, Evon P. Silvia, PLS, being duly registered as a Professional Land Surveyor in and by the state of Washington, hereby certify that the methodologies, static GNSS occupations used during airborne flights, and ground survey point collection were performed using commonly accepted Standard Practices. Field work conducted for this report was conducted between April 23 and 26, 2018.

Accuracy statistics shown in the Accuracy Section of this Report have been reviewed by me and found to meet the "National Standard for Spatial Data Accuracy".

Evon P. Silvia

Jul 19, 2018

Evon P. Silvia, PLS
Quantum Spatial, Inc.
Corvallis, OR 97330



SELECTED IMAGES

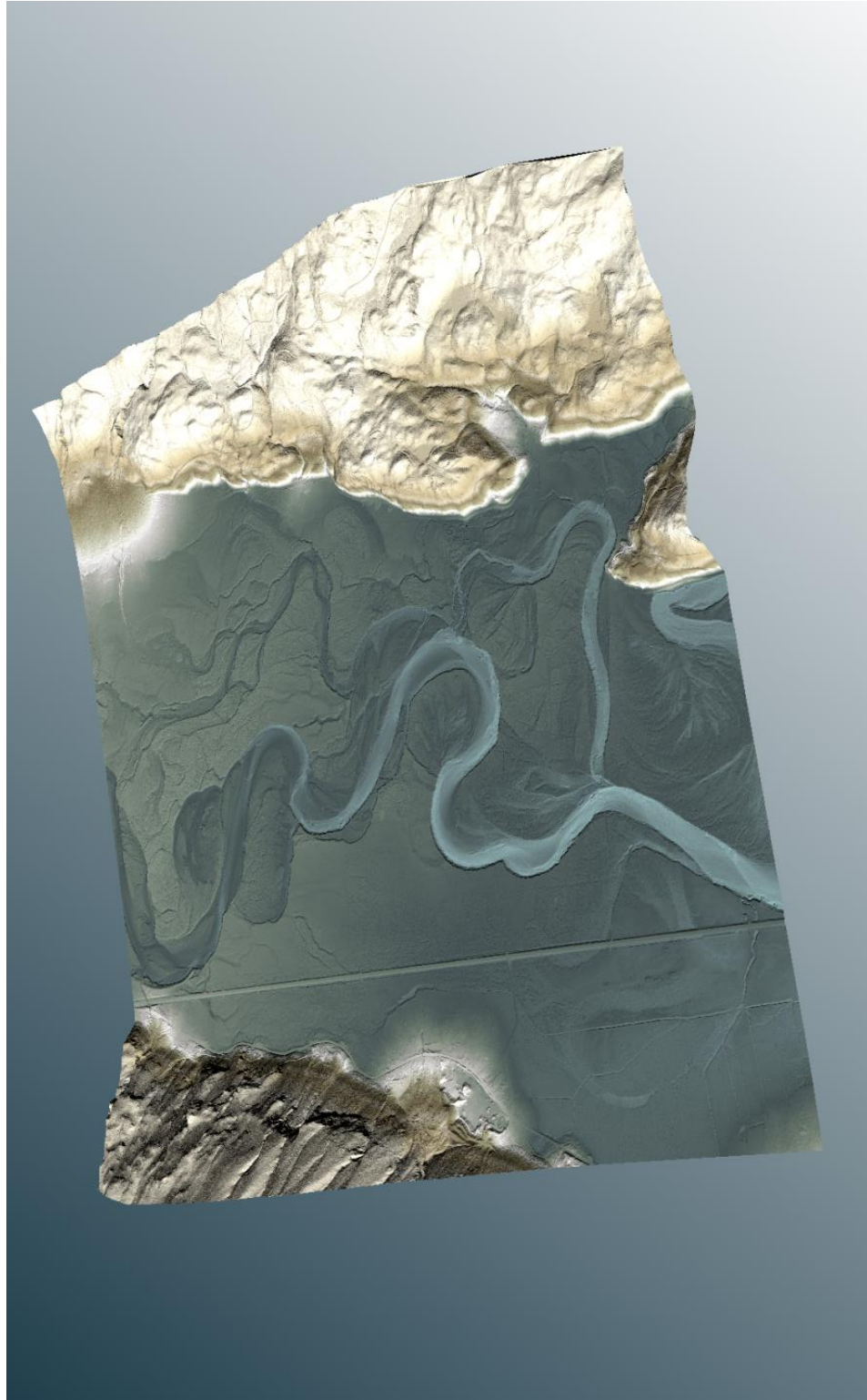


Figure 16: View looking east over Cowlitz River. The image was created from the LiDAR bare earth model and colored by elevation.

GLOSSARY

1-sigma (σ) Absolute Deviation: Value for which the data are within one standard deviation (approximately 68th percentile) of a normally distributed data set.

1.96 * RMSE Absolute Deviation: Value for which the data are within two standard deviations (approximately 95th percentile) of a normally distributed data set, based on the FGDC standards for Non-vegetated Vertical Accuracy (FVA) reporting.

Accuracy: The statistical comparison between known (surveyed) points and laser points. Typically measured as the standard deviation (sigma σ) and root mean square error (RMSE).

Absolute Accuracy: The vertical accuracy of LiDAR data is described as the mean and standard deviation (sigma σ) of divergence of LiDAR point coordinates from ground survey point coordinates. To provide a sense of the model predictive power of the dataset, the root mean square error (RMSE) for vertical accuracy is also provided. These statistics assume the error distributions for x, y and z are normally distributed, and thus we also consider the skew and kurtosis of distributions when evaluating error statistics.

Relative Accuracy: Relative accuracy refers to the internal consistency of the data set; i.e., the ability to place a laser point in the same location over multiple flight lines, GPS conditions and aircraft attitudes. Affected by system attitude offsets, scale and GPS/IMU drift, internal consistency is measured as the divergence between points from different flight lines within an overlapping area. Divergence is most apparent when flight lines are opposing. When the LiDAR system is well calibrated, the line-to-line divergence is low (<10 cm).

Root Mean Square Error (RMSE): A statistic used to approximate the difference between real-world points and the LiDAR points. It is calculated by squaring all the values, then taking the average of the squares and taking the square root of the average.

Data Density: A common measure of LiDAR resolution, measured as points per square meter.

Digital Elevation Model (DEM): File or database made from surveyed points, containing elevation points over a contiguous area. Digital terrain models (DTM) and digital surface models (DSM) are types of DEMs. DTMs consist solely of the bare earth surface (ground points), while DSMs include information about all surfaces, including vegetation and man-made structures.

Intensity Values: The peak power ratio of the laser return to the emitted laser, calculated as a function of surface reflectivity.

Nadir: A single point or locus of points on the surface of the earth directly below a sensor as it progresses along its flight line.

Overlap: The area shared between flight lines, typically measured in percent. 100% overlap is essential to ensure complete coverage and reduce laser shadows.

Pulse Rate (PR): The rate at which laser pulses are emitted from the sensor; typically measured in thousands of pulses per second (kHz).

Pulse Returns: For every laser pulse emitted, the number of wave forms (i.e., echoes) reflected back to the sensor. Portions of the wave form that return first are the highest element in multi-tiered surfaces such as vegetation. Portions of the wave form that return last are the lowest element in multi-tiered surfaces.

Real-Time Kinematic (RTK) Survey: A type of surveying conducted with a GPS base station deployed over a known monument with a radio connection to a GPS rover. Both the base station and rover receive differential GPS data and the baseline correction is solved between the two. This type of ground survey is accurate to 1.5 cm or less.

Post-Processed Kinematic (PPK) Survey: GPS surveying is conducted with a GPS rover collecting concurrently with a GPS base station set up over a known monument. Differential corrections and precisions for the GNSS baselines are computed and applied after the fact during processing. This type of ground survey is accurate to 1.5 cm or less.

Scan Angle: The angle from nadir to the edge of the scan, measured in degrees. Laser point accuracy typically decreases as scan angles increase.

Native LiDAR Density: The number of pulses emitted by the LiDAR system, commonly expressed as pulses per square meter.

APPENDIX A - ACCURACY CONTROLS

Relative Accuracy Calibration Methodology:

Manual System Calibration: Calibration procedures for each mission require solving geometric relationships that relate measured swath-to-swath deviations to misalignments of system attitude parameters. Corrected scale, pitch, roll and heading offsets were calculated and applied to resolve misalignments. The raw divergence between lines was computed after the manual calibration was completed and reported for each survey area.

Automated Attitude Calibration: All data were tested and calibrated using TerraMatch automated sampling routines. Ground points were classified for each individual flight line and used for line-to-line testing. System misalignment offsets (pitch, roll and heading) and scale were solved for each individual mission and applied to respective mission datasets. The data from each mission were then blended when imported together to form the entire area of interest.

Automated Z Calibration: Ground points per line were used to calculate the vertical divergence between lines caused by vertical GPS drift. Automated Z calibration was the final step employed for relative accuracy calibration.

LiDAR accuracy error sources and solutions:

Type of Error	Source	Post Processing Solution
GPS (Static/Kinematic)	Long Base Lines	None
	Poor Satellite Constellation	None
	Poor Antenna Visibility	Reduce Visibility Mask
Relative Accuracy	Poor System Calibration	Recalibrate IMU and sensor offsets/settings
	Inaccurate System	None
Laser Noise	Poor Laser Timing	None
	Poor Laser Reception	None
	Poor Laser Power	None
	Irregular Laser Shape	None

Operational measures taken to improve relative accuracy:

Low Flight Altitude: Terrain following was employed to maintain a constant above ground level (AGL). Laser horizontal errors are a function of flight altitude above ground (about 1/3000th AGL flight altitude).

Focus Laser Power at narrow beam footprint: A laser return must be received by the system above a power threshold to accurately record a measurement. The strength of the laser return (i.e., intensity) is a function of laser emission power, laser footprint, flight altitude and the reflectivity of the target. While surface reflectivity cannot be controlled, laser power can be increased and low flight altitudes can be maintained.

Reduced Scan Angle: Edge-of-scan data can become inaccurate. The scan angle was reduced to a maximum of $\pm 20^\circ$ from nadir, creating a narrow swath width and greatly reducing laser shadows from trees and buildings.

Quality GPS: Flights took place during optimal GPS conditions (e.g., 6 or more satellites and PDOP [Position Dilution of Precision] less than 3.0). Before each flight, the PDOP was determined for the survey day. During all flight times, a dual frequency DGPS base station recording at 1 second epochs was utilized and a maximum baseline length between the aircraft and the control points was less than 13 nm at all times.

Ground Survey: Ground survey point accuracy (<1.5 cm RMSE) occurs during optimal PDOP ranges and targets a minimal baseline distance of 4 miles between GPS rover and base. Robust statistics are, in part, a function of sample size (n) and distribution. Ground survey points are distributed to the extent possible throughout multiple flight lines and across the survey area.

50% Side-Lap (100% Overlap): Overlapping areas are optimized for relative accuracy testing. Laser shadowing is minimized to help increase target acquisition from multiple scan angles. Ideally, with a 50% side-lap, the nadir portion of one flight line coincides with the swath edge portion of overlapping flight lines. A minimum of 50% side-lap with terrain-followed acquisition prevents data gaps.

Opposing Flight Lines: All overlapping flight lines have opposing directions. Pitch, roll and heading errors are amplified by a factor of two relative to the adjacent flight line(s), making misalignments easier to detect and resolve.